

Principal role of fungi in soil carbon stabilization during early pedogenesis in the high Arctic

Juan Carlos Trejos-Espeleta^a, Juan P. Marin-Jaramillo^{a,1}, Steven K. Schmidt^b, Pacifica Sommers^b, James A. Bradley^{c,d,2}, and William D. Orsi^{a,e,2} Affiliations are included on p. 10.

Edited by James Tiedje, Michigan State University, East Lansing, MI; received February 7, 2024; accepted June 4, 2024

Climate warming is causing widespread deglaciation and pioneer soil formation over glacial deposits. Melting glaciers expose rocky terrain and glacial till sediment that is relatively low in biomass, oligotrophic, and depleted in nutrients. Following initial colonization by microorganisms, glacial till sediments accumulate organic carbon and nutrients over time. However, the mechanisms driving soil nutrient stabilization during early pedogenesis after glacial retreat remain unclear. Here, we traced amino acid uptake by microorganisms in recently deglaciated high-Arctic soils and show that fungi play a critical role in the initial stabilization of the assimilated carbon. Pioneer basidiomycete yeasts were among the predominant taxa responsible for carbon assimilation, which were associated with overall high amino acid use efficiency and reduced respiration. In intermediate- and late-stage soils, lichenized ascomycete fungi were prevalent, but bacteria increasingly dominated amino acid assimilation, with substantially decreased fungal:bacterial amino acid assimilation ratios and increased respiration. Together, these findings demonstrate that fungi are important drivers of pedogenesis in high-Arctic ecosystems that are currently subject to widespread deglaciation from global warming.

polar ecology | fungal ecology | climate change | Arctic soil | carbon cycle

Glaciers cover approximately 10% of land on Earth; however, almost all glaciers worldwide are losing mass at an accelerating rate (1). Climate warming is amplified in the Arctic (2), where glacier retreat is particularly rapid and widespread (3, 4). Following ice retreat, glacial deposits undergo pedogenesis (forming proglacial soils), and retreating glacier fronts therefore provide natural laboratories where varying stages of soil development can be observed simultaneously along a chronosequence (5–11).

Microorganisms are the pioneer colonizers of newly exposed proglacial soils, but the microbial communities are limited by the availability of the nutrients phosphorus (P) and nitrogen (N) in the earliest stages of soil formation (12-14). Nutrient-limited C- and N-fixing cyanobacteria and other photoautotrophs are major sources of organic C and N to the proglacial sediments and pioneer soils (15-17) as well as allochthonous delivery of organic C and N to the glacier forefield via glacier-fed streams (9). As proglacial soil develops over time, organic carbon and biomass increase leading to a greater amount of stored organic C and N (9, 12–14, 18). Soil formation in glacier forefields exemplifies not only the carbon storage potential of newly exposed terrain but also the recovery of soil ecosystems at the end of glacial periods and the onset of interglacial periods—since glacial retreat has been a consistent and widespread feature throughout Earth's past (19).

Bioavailable organic matter in pioneer soils of glacier forefields is subject to remineralization to CO₂ by microbial respiration—which controls the stability of organic C and N in the soil. Soil microorganisms largely control soil C storage and soil-atmosphere C exchange (20, 21), and it has been proposed that microbial carbon use efficiency (CUE) is one of the key parameters controlling how much carbon is sequestered and stored in soils (22). CUE can be defined as the fraction of the total carbon uptake by soil microorganisms that is assimilated into biomass, versus carbon that is respired as CO₂. High CUE values are associated with high allocation of C to biomass that sequesters C as soil organic carbon (22, 23). Natural microbial communities are complex and comprise taxa that grow and assimilate nutrients at different rates and different CUE under different conditions (24). Increasing the temperature of Arctic ecosystems is likely to stimulate microbial activity since many microbes live below their optimal growth temperature (25), but it is still poorly understood which microbes will be more or less critical for organic carbon storage under altered conditions.

Fungal traits in soil can play a key role in promoting carbon storage in soils (26). The ratio of fungi to bacteria, also referred to as the fungal:bacterial ratio (F:B ratio), is an

Significance

Glaciers cover approximately 10% of land on Earth and are in rapid decline due to climate warming. As glaciers melt and retreat, they expose new bedrock and terrain that over time transforms into soil. Microbes are responsible for controlling how much carbon is stored in the newly developed soils, but how microbial activity promotes carbon storage under these conditions is poorly understood. We report that fungi in a high-Arctic glacial ecosystem drive carbon stabilization in soils within decades after glacier retreat. The pioneer fungi taxa most important for promoting carbon storage were black yeasts. Our results show that fungi will play a critical role in future Arctic soil carbon storage, as glaciers continue to shrink and expose more terrain.

The authors declare no competing interest.

This article is a PNAS Direct Submission.

Copyright © 2024 the Author(s). Published by PNAS. This article is distributed under Creative Commons Attribution-NonCommercial-NoDerivatives License 4.0

Although PNAS asks authors to adhere to United Nations naming conventions for maps (https://www.un.org/ geospatial/mapsgeo), our policy is to publish maps as provided by the authors.

¹Present address: School of Architecture, Civil and Environmental Engineering (ENAC), École Polytechnique Fédérale de Lausanne, Switzerland, 1015 Lausanne.

²To whom correspondence may be addressed. Email: jbradley.earth@gmail.com or w.orsi@lrz.uni-muenchen.de.

This article contains supporting information online at https://www.pnas.org/lookup/suppl/doi:10.1073/pnas. 2402689121/-/DCSupplemental.

Published July 2, 2024.

important predictor of soil carbon storage because higher F:B ratios generally correspond with increased soil C storage (27–32). The F:B ratio is based on the fact that bacteria and fungi are two distinct and major decomposer groups in soils (32), and low F:B ratios have been found to be associated with increased respiration and decreased carbon storage capacity (29). Increased fungal activity is suggested to enhance organic C accumulation (33) and stabilize soil organic C via an increased CUE by fungi compared to bacteria (28, 30, 34). Although fungi are prevalent in pioneer soils (35, 36), their role in driving carbon storage and availability during pedogenesis of glacial deposits is not known. High-Arctic ecosystems have a uniquely high diversity of fungi relative to plants (37), in stark contrast to low latitudes—raising the possibility that fungal communities might serve a key role as ecosystem engineers. Knowledge of carbon assimilation processes of fungal and bacterial populations and how this relates to ecosystem carbon flux is critical to understand and predict how terrestrial ecosystems in the Arctic will respond to future warming and how they may have responded to past periods of environmental change. The magnitude and efficiency of organic carbon assimilation of individual fungal taxa and groups may indicate how they impact soil C and N storage in developing soils as Arctic temperatures rise and may also shed light on key initial stages of terrestrial ecosystem recovery after deglaciation events.

To address the role of fungi in Arctic soil development, we traced organic carbon and nitrogen uptake by microorganisms in newly exposed glacial deposits in the forefield of a retreating glacier in Svalbard in the High-Arctic. Here, ice-free terrestrial environments are expanding at an exceptionally high rate, and these areas are subject to colonization by microbes and plants, which enhance biogeochemical cycling (9). We quantified fungal C assimilation by specific fungal taxa using ¹³C-labeled amino acids in quantitative stable isotope probing incubations (qSIP) of soils from three different stages of soil development along a proglacial chronosequence. DNA quantitative stable isotope probing (qSIP) is a technique that can elucidate quantitative assimilation of a given substrate by specific bacterial (24) and fungal (38) taxa. We chose amino acids as a tracer for fungal organic carbon cycling because amino acids are an important substrate for Arctic soil microbes (39-41). Amino acids are a major component of glacially derived dissolved organic matter (42, 43) that is delivered to the glacier forefield via glacier-fed streams, and amino acid uptake and assimilation by fungi is an important control on soil carbon storage and nitrogen immobilization (26). In addition to fungal amino acid assimilation, we also quantified bacterial assimilation of amino acids using DNA-SIP and assessed F:B amino acid assimilation ratios. By assessing not only the F:B ratio in terms of biomass but also F:B amino acid assimilation, we quantitatively assess how amino acid assimilation in fungi compares to bacteria at different stages of soil development. All SIP incubations were combined with measurements of ¹³C in respired CO₂ to investigate relationships between F:B amino acid assimilation ratios and soil respiration, which provides insight into how fungal activity influences carbon cycling at different stages of ecosystem recovery and development.

Results and Discussion

Soil Succession in the Chronosequence. The Midtre Lovénbreen chronosequence first described by Hodkinson et al. (17) proceeds from the glacier snout with several hundred meters of glacial till with no to little plant cover, followed by moraines (Fig. 1) with scattered mosses and lichens, followed by grasses and flowering plants in more mature stages of soil development. Total organic

carbon (TOC), total nitrogen (TN), and total adenylate (ATP+ADP+AMP) concentrations (as a measure of total microbial biomass) were variable along the chronosequence (Fig. 2) but show a general accumulation of nutrients (TOC and TN) and microbial biomass (total adenylate) after the glacier snout (Fig. 3). Most of the increase in TOC, TN, and total adenylate was observed within the first few decades of soil formation, which is relatively stable across the remainder of the chronosequence (Fig. 2) and displays increased median values in the tundra soils after the terminal moraine (Fig. 3). These trends in total biomass, TOC, and TN are largely consistent with prior observations from the Midtre Lovénbreen chronosequence showing an increase in plant cover and microbial biomass with increasing soil age (17, 44).

The bacterial and fungal biomass estimated by qPCR covary and correlate positively with one another across many geomorphological features throughout the proglacial soil chronosequence (Spearman Rho = 0.93, P < 0.01, Fig. 2 and SI Appendix, Fig. S1A), indicating that the abundance of bacteria and fungi is tightly coupled across the entire chronosequence and both bacteria and fungi are shaped and limited by similar factors. The concentration of fungal 18S rRNA genes was consistently 1 to 2 orders of magnitude lower than the concentration of bacterial 16S rRNA genes. Fungal and bacterial biomass were lowest in the youngest soils immediately in front of the glacier (fungi: 10⁶ 18S rRNA gene copies g⁻¹; bacteria: 10⁷ 16S rRNA gene copies g⁻¹). Bacterial 16S rRNA gene abundance increased notably in the earliest stages of development, reaching a plateau in soils approximately 30 years old (at 10⁹ 16S rRNA gene copies g⁻¹) (Fig. 2). In contrast, fungal 18S rRNA gene abundance is slower to reach a plateau—occurring in soils ca. 50 y old (at 10⁸ fungal 18S rRNA gene copies g⁻¹) (Fig. 2). After 50 y of soil development, bacterial and fungal 18S rRNA gene abundance varies across the chronosequence with intermittently lower values until the terminal moraine but generally remains at or below the concentrations observed at 30 or 50 y of development, respectively (Fig. 2). In the older tundra soils (>120 y), located outside the terminal moraines (Fig. 1), the concentration of fungal 18S and 16S rRNA genes is relatively constant (Fig. 2). These findings are generally consistent with observations that the accumulation of nutrients in proglacial soils is accompanied by increased microbial biomass and activity (45, 46).

We assessed the diversity of bacterial communities via 16S rRNA gene sequencing which showed the glacier and glacier snout communities are dominated by Gammaproteobacteria, Cyanobacteria, and Bacteroidetes, whereas the communities in the young soils directly in front of the glacier (ca. 10 y old) have a higher relative abundance of Alphaproteobacteria and lower relative abundance of Cyanobacteria (Fig. 2D). Chloroflexi, Acidobacteria, Planctomycetes, and Actinobacteria increase in relative abundance to become dominant in 30-y-old soils. After 50 y, the major bacterial groups do not exhibit substantial changes in relative abundance, except for Chloroflexi which shows variability correlating positively with TOC (Spearman Rho = 0.556, P < 0.001) (Fig. 2). Overall, our results are consistent with previous surveys of this forefield (17) and other proglacial chronosequences (47, 48).

The diversity of fungi was assessed using high-throughput sequencing of the internal transcribed spacer region 1 (ITS1), a marker for fungal taxonomic identifications (49), which showed that the fungal communities on the glacier and glacier snout are significantly different from the proglacial soil (ANOSIM R = 0.9829, P = 0.001) and were dominated by Microbotryomycetes (Basidiomycota) (Fig. 2*D*). This is consistent with general observations that glacier associated fungal communities tend to be dominated by Microbotryomycetes and other cold-adapted basidiomycete yeasts (50–57) that are selected for under the extremely

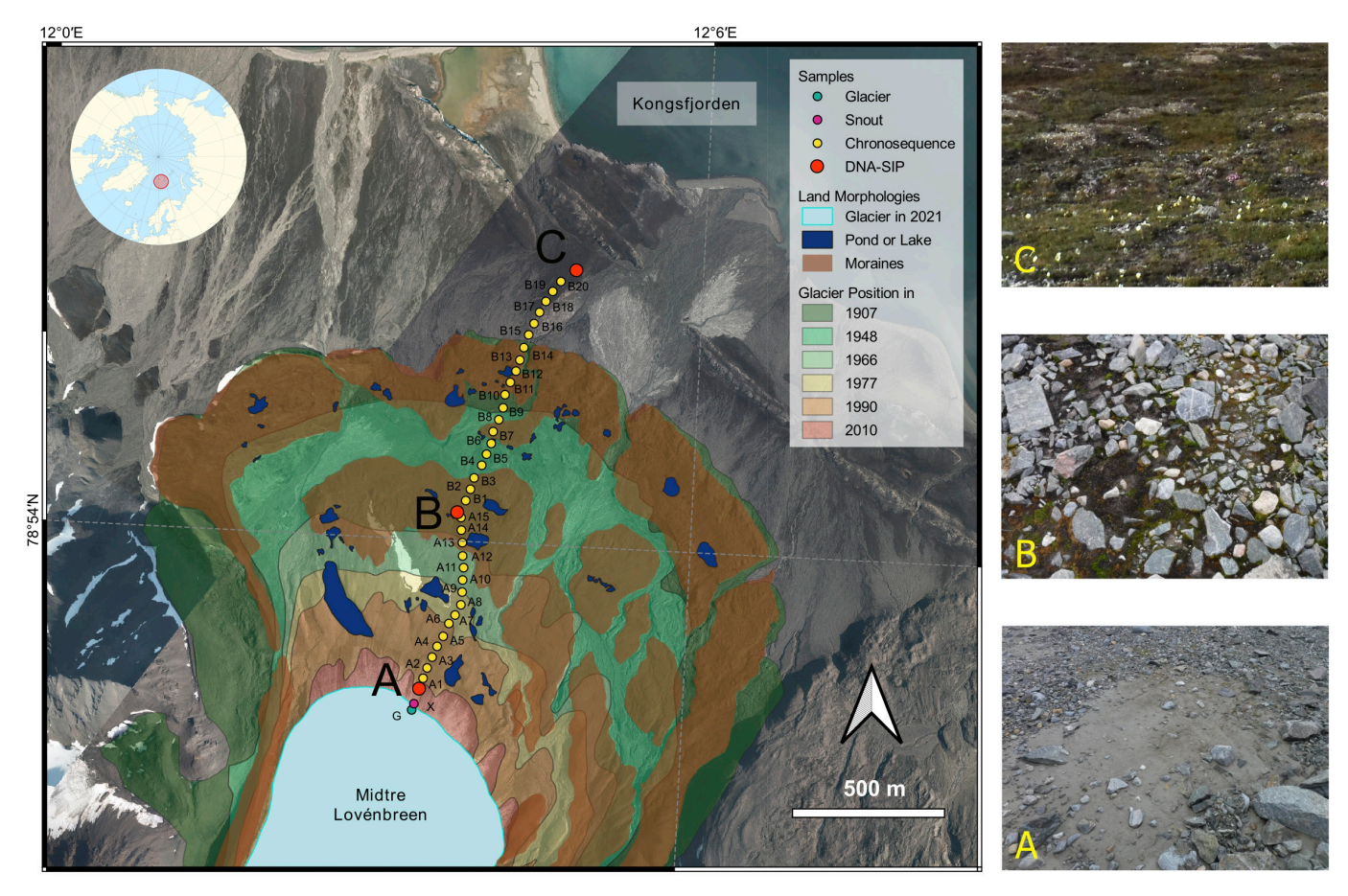


Fig. 1. Aerial view of the Midtre Lovénbreen glacier forefield and chronosequence sampling transect showing locations for SIP incubations. The photo of Midtre Lovénbreen's forefield on the West coast of Spitsbergen, Svalbard, is a satellite image from the Norwegian Polar Institute. Glacier front lines and their respective ages over the last century were obtained from the published estimates of Bourriquen et al. (2018) according to the Norwegian Polar Institute data. Right: Photographs of sites A (proglacial rock flour sediment), B (rocky, intermediate soils), and C (developed tundra soils) where the stable isotope probing (SIP) incubations were performed.

cold conditions of the high-Arctic (58) possibly as a result of yeast stress-tolerance traits (26). The fungal community changes dramatically in the glacier snout till sediment (site A) to become overwhelmingly dominated by taxa affiliated with the basidiomycete group Moniliellomycetes (81% of total fungal ITS reads) (Fig. 2D). The dominance of Moniliellomycetes (Basidiomycota) in proglacial sediments is constrained to site A0, 40 m from the snout of the glacier, and is consistent with basidiomycetes fungi dominating the glacier associated mud (n = 3) and glacial snout (n = 3) sediments immediately adjacent to this site, prior to the onset of pedogenesis. Beyond site A1, the Leotiomycetes (Ascomycota) replaces Moniliellomycetes as the dominant fungal group after only 10 y of soil development (increasing from 5 to 87%). In older soils (>30 y), the fungal community gradually becomes dominated by lichenizing groups of Eurotiomycetes (57.5 ± 26.6%) (Fig. 2D). Our observations are consistent with previous reports of stark differences between glacial (cryoconite) and soil (moraine and tundra) fungal communities (55) and increased fungal diversity with increasing stages of soil development (59). The differing rates of fungal and bacterial community assemblies seen here (Fig. 2) could be attributed to environmental filtering and selection whereby fungi and bacteria respond differently to the various physicochemical factors along the transect (7, 8) and/or that bacteria have a more cosmopolitan distribution than fungi in this particular region of Svalbard (53).

The fungal community appears to switch from being dominated by oligotrophic, psychrophilic basidiomycete yeasts in the glacier and proglacial sediment, toward lichenizing fungi in the more

developed soils. In the early stages of soil development, the basidiomycete yeasts (Microbotryomycetes and Moniliellomycetes) that dominated the glacier and glacial snout sediments (Fig. 2D) are likely sourced from supra- and subglacial environments (60, 61). The Moniliellomycetes OTUs in sites A and A1 are dominated by the genus Moniliella, a group of black yeasts, and appear to represent key pioneer fungi, that are quickly replaced by Ascomycota (Leotiomycetes) within a matter of decades (Fig. 2). The transition of fungal communities in more developed soils could be explained by the development of plant root systems (46), that are associated with mediation of carbon and nitrogen cycling (62) and increased nutrient availability (18). This is a likely factor explaining the increase in fungal abundance for the first several decades along the chronosequence and the fungal community succession toward lichenizing Eurotiomycetes in the later stages of the chronosequence where soils have denser coverage of mosses and plants (17) (Fig. 2).

Geomorphological features along the transect were used to group the samples into the following gradient classes: glacier, snout, early soils, inner moraine, intermediate soils, terminal moraine, and tundra (Figs. 1 and 2). Grouping the transect sites into gradient classes, the ratio of bacterial 16S to fungal 18S rRNA genes shows that the fungi:bacteria ratios (F:B ratios) are higher on the glacier and in the rock flour sediments at the glacier "snout," compared to the older soils of the chronosequence (Fig. 3 and SI Appendix, Fig. S1B). Also, the median F:B ratio of the youngest section of the proglacial chronosequence is higher than the intermediate soils (Fig. 3). The elevated F:B ratios on the glacier and

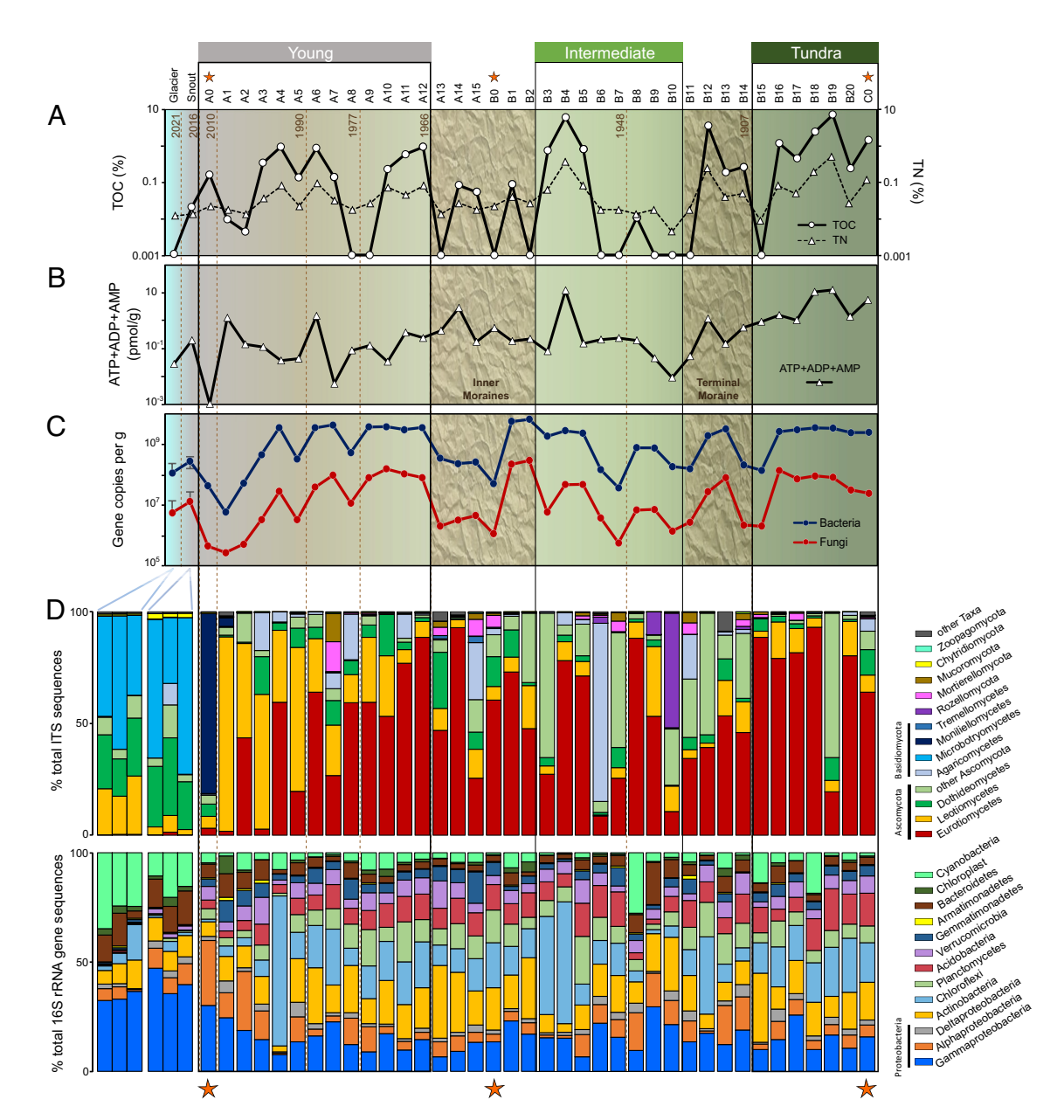


Fig. 2. Biomass accumulation and microbial community assembly across a 100-y soil Arctic proglacial soil chronosequence. (*A*) Total organic carbon (TOC) and total nitrogen (TN) concentrations. The detection limit for TOC and TN was 0.001%. DL: detection limit. (*B*) Total adenylate (ATP+ADP+AMP) concentration. (*C*) Concentrations of bacterial 16S (blue) and fungal 18S (red) rRNA gene copies. (*D*) Relative abundance of major taxonomic groups within 16S rRNA gene and fungal ITS datasets. For the glacier and snout, three replicates were taken and are displayed at the left of the chronosequence. The orange stars indicate the sites where SIP incubations were conducted. Glacier front lines, their respective ages over the last century, were obtained from the published estimates of Bourriquen et al. (2018) according to the Norwegian Polar Institute data.

in the youngest proglacial sediments raised the possibility that these early successional sites may have relatively higher potential for increased carbon storage (27–32).

To better understand the ecological role of fungi in pioneer soil development and soil carbon cycling and stabilization, we performed DNA-SIP incubations with a mixture of 17 ¹³C-labeled amino acids from three sites representing initial, intermediate, and developed soils (sites A, B, and C) (Fig. 1).

Amino Acid Assimilation by Fungi and Bacteria. Using qPCR to quantify bacterial and fungal rRNA gene distributions across density gradients (*SI Appendix*, Fig. S2), we could determine buoyant density shifts, and calculate the ¹³C-excess atomic fraction (EAF) of 16S and fungal 18S rRNA genes (Fig. 4). We found that fungi in the least-developed soils immediately adjacent to the retreating glacier snout (site A) had higher rates of amino acid

assimilation than the fungi in older, more developed soils (sites B and C). The highest fungal ¹³C-EAF in fungal 18S rRNA genes across the entire chronosequence was observed in the earliest pioneer soils (site A), reaching ¹³C-EAF values >50% (Fig. 4). Here, the fungal 18S rRNA genes were labeled in all three SIP incubations tested after 7 d (median fungal EAF: 15%), including those with added kaolinite and montmorillonite (albeit threefold to 20-fold less compared to the control) (Fig. 4)—indicating high rates of fungal activity. At site B (inner moraine), no fungal amino acid assimilation was detected; rather, bacteria were observed to assimilate amino acids in every SIP incubation at this site (Fig. 4). The dominance of bacterial amino acid assimilation over fungi at site B may be due to an increased competition between bacteria and fungi in the intermediate soils and that bacteria are more limited by amino acids at this site compared to fungi. In the tundra soil, fungal amino acid assimilation after 1 day was comparable to bacteria

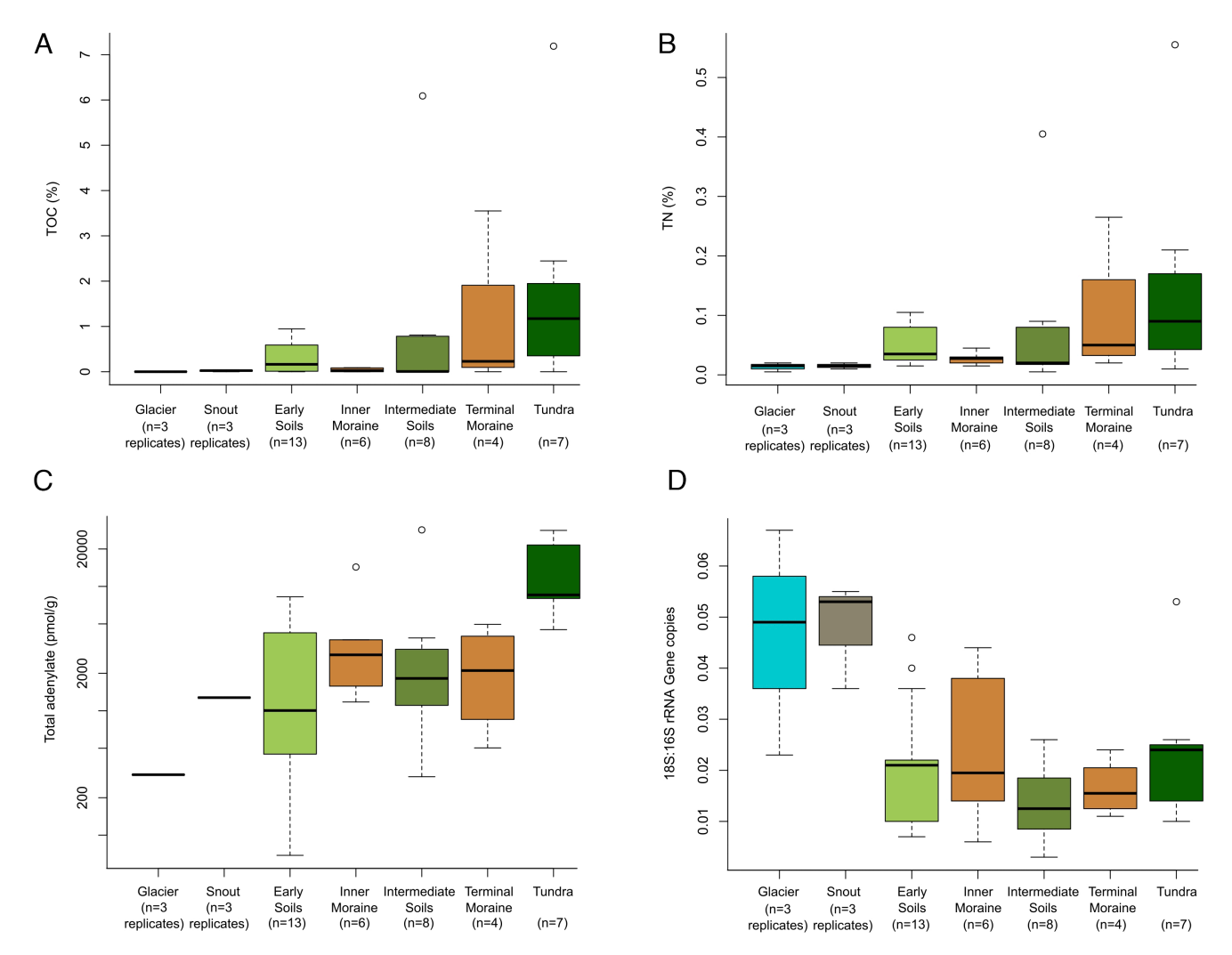


Fig. 3. Boxplots of soil biochemistry and microbial biomass by soil succession stage. (A) Total organic carbon concentrations (TOC %). (B) Total nitrogen concentrations (TN %). (C) Total adenylate concentrations (ATP+ADP+AMP). (D) F:B ratios based on qPCR quantification of rRNA gene concentrations (fungal 18S:16S). The samples are derived from a single transect and grouped into the gradient classes based on age estimates and large-scale geomorphological features (Fig. 1). The glacier and snout classes had three biological replicates, whereas all other groups derive from single samples along the transect grouped into geomorphological features.

(fungal EAF: 19%; bacterial EAF: 31%), and fungal amino acid assimilation was higher than bacteria after seven days in tundra soils incubated with montmorillonite-amended amino acids (Fig. 4).

Rates of microbial amino acid assimilation in soil uptake experiments are impacted by incubation conditions, namely moisture and concentration of the added amino acids (40). The soils and sediments investigated here are located in a hydrologically dynamic glacial forefield that experiences large seasonal fluctuations in moisture due to precipitation and glacier-fed streams (17) and so additional moisture in the SIP incubations was reflective of conditions that the microbes are naturally exposed to. The kinetics of amino acid uptake in soils are controlled by the concentration of amino acids added (40) and so the addition of amino acids probably increased rates relative to the in situ state at the time of sampling. To reduce excessive alteration of the system, we added the amino acids at a concentration <5% of the natural TOC concentration (Fig. 2A). The concentrations of amino acids in our incubations were roughly three times lower compared to a previous study in agricultural soil that measured bacterial amino acid assimilation with DNA-SIP (63). Nevertheless, for the reasons outlined above, we interpret assimilation rates with caution and only consider them to be potential rates. Our results are in general agreement with other

soil amino acid uptake studies showing that some soil fungi can quickly respond to local increased addition of amino acids (40).

Compared to the fungi, we found evidence of bacterial amino acid incorporation in all sites, with mean ¹³C-EAF values (in 16S rRNA genes) of 43% at site A (including those with additional kaolinite and montmorillonite clay minerals), 9% at site B, and 11% at site C (Fig. 4 and SI Appendix, Fig. S2). This is consistent with prior DNA-SIP studies that found that when exposed to fresh amino acid additions, many soil bacteria can assimilate ¹³C-labeled amino acids into DNA relatively quickly (63, 64).

Amino acid assimilation was dominated by fungi in the least-developed (i.e., pioneer) soils (site A) and by bacteria in intermediate and developed soils (sites B and C, respectively) (Fig. 4). Bacteria had higher EAF values than fungi in most (82%, n = 11) of the SIP incubations, which might be related to the fact that bacteria have a higher amino acid uptake affinity compared to fungi (40). In general, rates of ¹³CO₂ respiration from amino acids were highest when amino acid assimilation was dominated by bacteria rather than by fungi (Fig. 4). This suggests that fungi in early-stage soils may assimilate organic carbon and nitrogen more efficiently than bacteria in later-stage soils and that the proglacial soil fungi may have higher CUE compared to bacteria. Site A Site B Site C

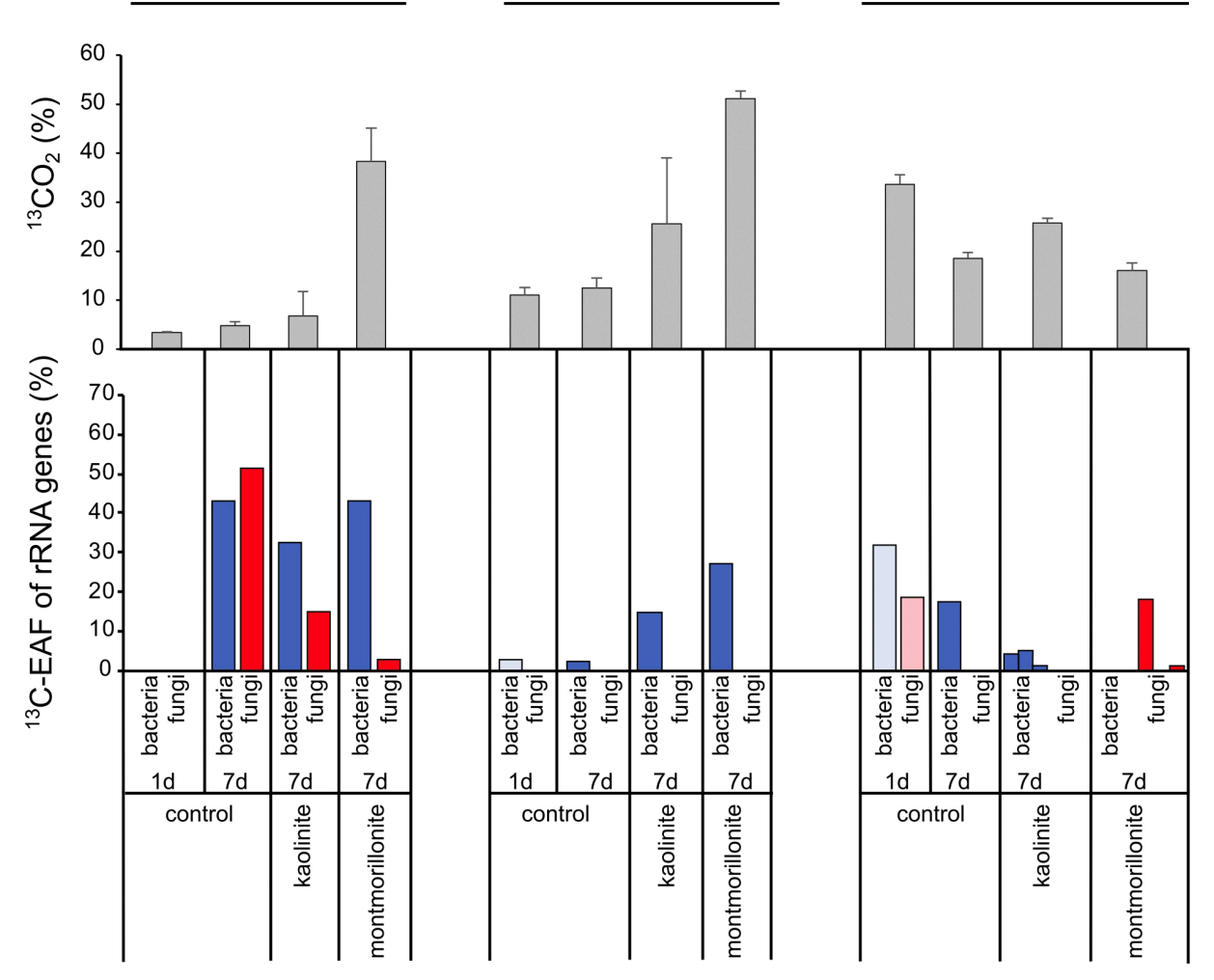


Fig. 4. Fungal ¹³C excess atomic fraction (¹³C-EAF), bacterial ¹³C-EAF, and ¹³C-labeled CO₂ production across the chronosequence. *Top* panel: The percentage of ¹³C-labeled CO₂ at the end of the SIP incubations. Shaded bars and error bars represent average and SDs from three technical replicates. *Bottom* panel: ¹³C-EAF values for fungal 18S (red) and bacterial 16S (blue) rRNA genes. Control: ¹³C-labeled amino acid addition with no added clay minerals. Kaolinite: ¹³C-labeled amino acids supplemented with kaolinite. At the tundra site C, three technical replicates for DNA density gradient fractionation were performed for the kaolinite and montmorillonite stable isotope probing (SIP) incubations that are represented by three individual bars.

This observation fits with predictions of increased CUE by stress-tolerant yeasts adapted to extreme environments that can promote enhanced soil C storage (26). Our finding of higher CO₂ production rates in more developed soils is consistent with alpine proglacial ecosystems that transition from CO₂ sinks to sources with decreasing glacier coverage and an increase in vegetation (65).

Fungal:Bacterial Amino Acid Assimilation (EAF) Ratios. In order to assess how ratios of fungal to bacterial carbon assimilation relate to respiration, we used the 13 C-EAF values of fungal 18S and bacterial 16S rRNA genes (Fig. 4) to calculate F:B EAF ratios. Across all of the incubations performed, at the three different successional sites, the F:B EAF ratio correlates negatively with 13 CO₂ production from respiration (Fig. 5) (Spearman Rho = 0.657, P = 0.024, $R^2 = 0.5159$, P = 0.005). This shows that in the pioneer soils where fungi dominated the amino acid assimilation (relative to bacteria), there was less remineralization of amino acids and a higher assimilation of amino acids into biomass. In contrast, when bacteria dominated amino acid assimilation (relative to fungi) there was more CO₂ produced from amino acids. The negative correlation between respiration and F:B EAF

ratio (Fig. 5) strongly suggests a higher fungal amino acid CUE and consequently increased soil carbon stabilization as biomass. Incubations from the proglacial rock flour sediments (not containing additional clay minerals) exhibited the highest F:B EAF ratios and the lowest $^{13}\mathrm{CO}_2$ production (Fig. 5), indicating that pioneer fungi promote carbon storage and stabilization. As glacier coverage decreases, proglacial ecosystems transition from CO_2 sinks to sources (65), and our findings indicate that fungi play a critical role in the early stages of pedogenesis and carbon stabilization shortly after glacier retreat.

Our findings are consistent with temperate fungal–bacterial carbon turnover dynamics where increased F:B ratios also correlate with decreased respiration and increased C storage (27) and low F:B ratios that were associated with increased respiration and decreased carbon storage capacity (30). The higher F:B EAF ratios at site A (Fig. 5) immediately adjacent to the snout are consistent with higher F:B biomass ratios in the glacier and snout sediments and the younger proglacial sediments (Fig. 3). These results prompted us to investigate which fungal taxa were responsible for the high F:B EAF ratios in the pioneer soils to establish quantitative links between key fungal taxa and carbon cycling processes.

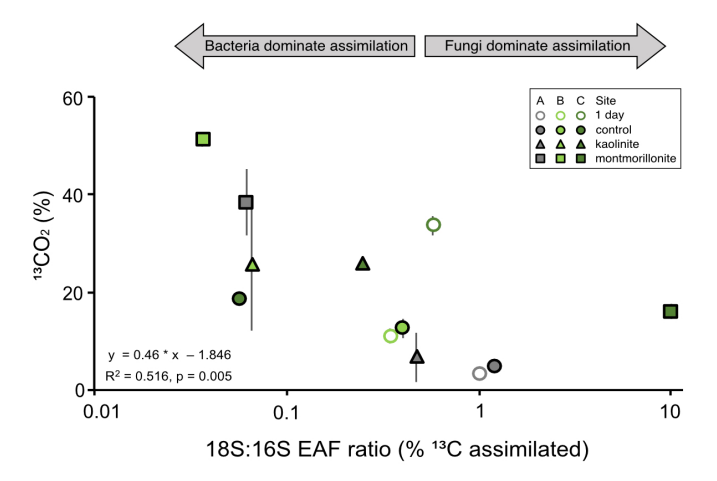


Fig. 5. Remineralized $^{13}CO_2$ as a function of the fungal:bacterial (18S:16S) ^{13}C excess atomic fraction ($^{\bar{13}}C$ -EAF) ratio. The x axis represents the ratio of fungal 18S rRNA ¹³C-EAF compared to the bacterial 16S rRNA ¹³C-EAF in the respective ¹³C-labeled amino acid SIP incubations. The y axis indicates the % of CO₂ that contained the ¹³C label; error bars represent SDs. Open circles represent 1-d control SIP incubations with no clay minerals added. Filled symbols represent 7-d SIP incubations. Circles: ¹³C-labeled amino acid with no clay minerals added; triangles: ¹³C-labeled amino acids with additional kaolinite; squares: 13C-labeled amino acids with additional montmorillonite. Note that increased F:B ¹³C-EAF ratios (18S:16S EAF ratio) are correlated with decreased $^{13}CO_2$ production.

Fungal Taxon-Specific Amino Acid Assimilation. To identify the key fungal taxa responsible for amino acid cycling with qSIP, we chose the two SIP incubations that had the highest ¹³C-EAF in

fungal 18S rRNA genes from youngest (glacier snout, site A; 7-d incubation with no mineral addition) and oldest (tundra, site C; 7-d incubation with montmorillonite) sites. Due to the low fungal biomass at site A (Fig. 2), the amount of extractable DNA was only sufficient for a single SIP replicate, and therefore, a quantitatively normalized Tag-SIP protocol ("Tag-qSIP") was performed (see Methods) to identify the labeled fungi and estimate their ¹³C-EAF values. In the tundra soil (site C), fungal biomass was higher (Fig. 2) and the amount of extractable DNA was sufficient to allow for replicates, and thus, qSIP could be applied (24). At the tundra site (site C), there was sufficient DNA extracted to allow for multiple ultracentrifugation replicates that were used as technical replicates for qSIP. The qSIP therefore was performed as previously described (66, 67) on three technical replicates of density gradient fractionated DNA extracted from the tundra SIP incubations. This allowed us to assess technical variation in shifts of DNA buoyant density between labeled treatments and unlabeled controls.

The recently exposed rock flour sediments (site A0) and the more developed tundra soils (site C) differ in fungal taxon-specific amino acid assimilation (Fig. 6), both in the magnitude and the identity of key active taxa. In the youngest soil (site A0), fungal OTUs exhibited on average higher EAF (52.90 ± 20.38 %), with five OTUs associated with the dominant basidiomycetes genus Moniliella (Moniliellomycetes) showing the highest rates of carbon assimilation (up to 100% 13 C EAF) (Fig. 6). The OTU clustering results of the fungal ITS1 data from the Tag-SIP incubations and chronosequence data revealed that the Moniliella affiliated OTUs that assimilated relatively high amounts of amino acids in the SIP incubations (Fig. 6) were the same fungal OTUs that dominated

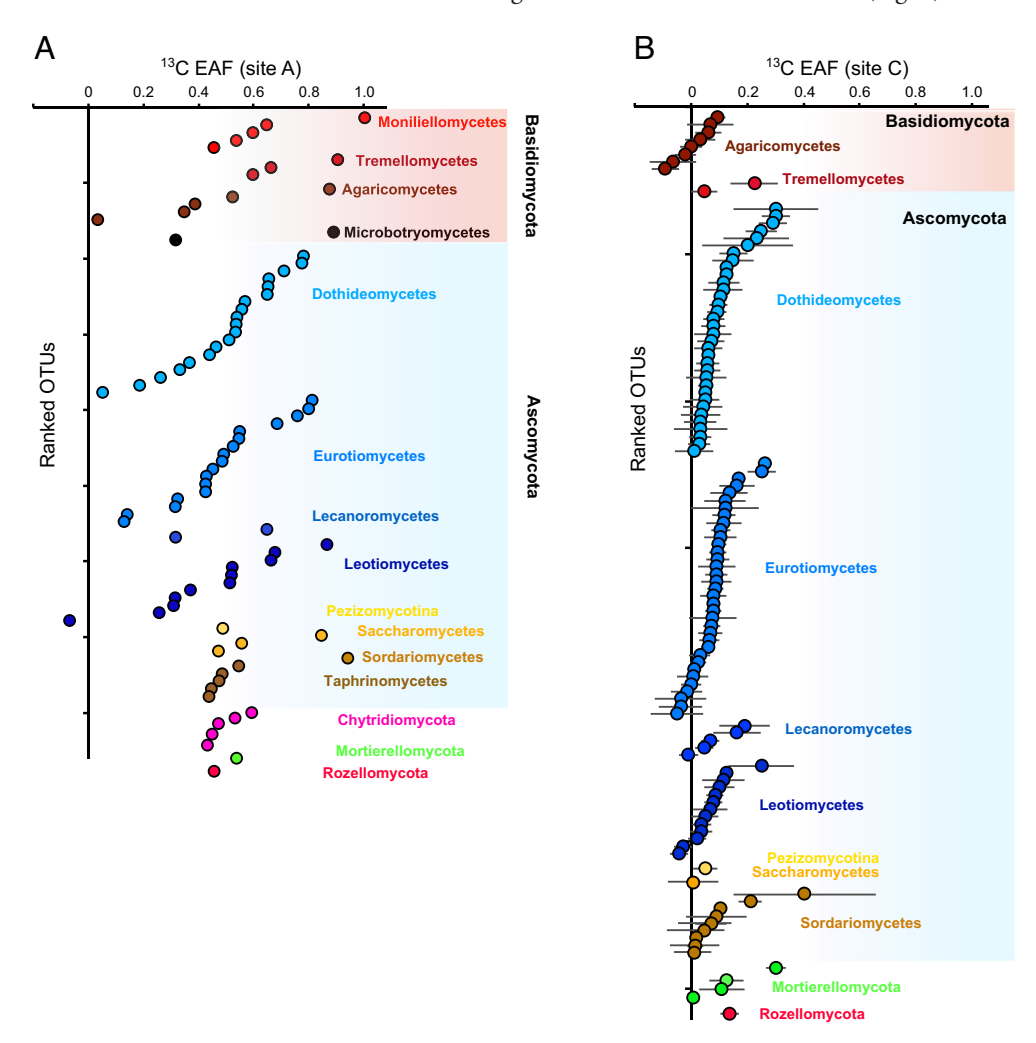


Fig. 6. ¹³C excess atomic fraction (¹³C-EAF) values for specific fungal taxa in proglacial sediments (panel A) and Arctic tundra (panel B). Individual points represent fungal OTUs, and their respective ¹³C-EAF values are represented by the x axis. For the tundra sample, bars correspond to the SD across three DNA density gradient fractionation replicates (technical replicates) from the stable isotope probing (SIP) incubation.

the proglacial soils at site A0 (Fig. 2D). These Moniliellomycetes affiliated OTUs corresponded to 28% and 63% of the total ITS1 sequences in the fungal community at the end of the ¹³C-labeled amino acid and unlabeled control incubations at site A0, respectively. Notably, a single *Moniliella*-affiliated OTU with 100% ¹³C-EAF (Fig. 6) represented 49% of the total ITS1 sequences at the end of the SIP incubations. This relatively high abundance of ¹³C-labeled Moniliellomycetes affiliated OTUs in the ¹³C-labeled and control SIP incubations at site A0 supports the fungal chronosequence data, indicating that the Moniliellomycetes are a dominant group in the earliest proglacial soils at this site (Fig. 2).

Moniliella is a genus of basidiomycete black yeasts (68) that have been reported from a relatively small number of environments predominantly human-affected ecosystems such as industrial and agricultural settings but have also been isolated from flowers in tropical rainforests (68–70). Our results show that a *Moniliella* sp. was the most important ecosystem engineer in the initial stages of soil development—and thus, our study expands the known ecological role of this genus to including soil carbon storage in the high-Arctic. Some Moniliella species are considered to be xerophilic and therefore can tolerate extreme dry conditions with low water activity (68-70). These traits would help to explain why fungi affiliated with the Moniliella dominate the fungal community in the early stages of the proglacial chronosequence (Fig. 2), which experience frequent wetting and drying, as well as freeze-thaw. While psychrophilic and oligotrophic basidiomycete yeasts tend to dominate fungal communities in polar ecosystems (51–54), our results show an important ecological function of psychrophilic Moniliella taxa for soil carbon stabilization in the cryosphere.

In the Tag-qSIP results from sediments adjacent to the glacier snout (site A), several Microbotryomycetes affiliated OTUs (*Yamadamyces* sp. and *Phenoliferia* sp.) had high ¹³C-EAF (88.8% and 31.5%, respectively). These basidiomycete yeast taxa dominated the glacier-associated fungal community but were in relatively low abundance at site A (Fig. 2D) where the SIP incubation was performed—only 40 m from the glacier snout (Fig. 1). Their high ¹³C-EAF (Fig. 6) compared to their low in situ abundance at site A (Fig. 2) indicates that their activity in proglacial sediments, after being transported from the glacier, might be limited in part by amino acids (or labile organic carbon in general).

Our results show that the ability of cold-adapted basidiomycete yeasts to assimilate amino acids is an important trait contributing to carbon stabilization in the high-Arctic ecosystem. A large number of psychrophilic yeasts and yeast-like fungi affiliated with the Microbotryomycetes have been isolated into pure culture from high-Arctic glacial environments, with some strains exhibiting dimorphic filamentous growth and rudimentary pseudohyphae (51). Psychrophilic Microbotryomycetes yeasts that were isolated from Arctic glacial environments were found to be able to assimilate a wide range of simple to complex sugars and polysaccharides, as well as amino acids (51). Melanin pigmentation is another common trait in polar basidiomycete yeasts (71) that may contribute to early soil carbon stabilization in proglacial soils because melanin from fungal necromass stabilizes soil organic matter (72). Therefore, an increased contribution of melanin containing psychrophilic basidiomycete yeasts to the necromass carbon pool in the proglacial sediments could be an additional fungal trait promoting early soil and carbon stabilization.

In the tundra, no basidiomycete Microbotryomycetes or Moniliellomycetes fungal OTUs were found to assimilate amino acids (site C, Fig. 6) indicating that the amino acid assimilating fungi in the tundra were distinct compared to the proglacial soils. Additionally, the amino acid assimilating fungi in the tundra have on average lower ¹³C-EAF values compared to the

proglacial sediment fungal taxa and are instead dominated by Ascomycota (Sordariomycetes, Dothideomycetes, Leotiomycetes, and Eurotiomycetes) (Fig. 6). The fungal OTU with the highest EAF in the tundra qSIP incubations was affiliated with the genus *Mrakia* (EAF: 22.4 ± 8.4%) (Fig. 6). Cold-adapted yeasts from the genus *Mrakia* (Tremellomycetes) are often isolated from polar and alpine cryosphere habitats (73), consistent with their high rates of amino acid assimilation in the tundra soils seen here. Fungi are known to have differences in amino acid uptake affinities between species (40), and this may explain in part the different levels of amino acid assimilation observed between fungal taxa that we observed in the qSIP results.

Influence of Clay Minerals on Amino Acid Assimilation. We added clay minerals to SIP incubations at each of the three sites (Fig. 1) because sorption onto clay mineral surfaces is predicted to reduce the bioavailability of organic C and N in soils (74) and is hypothesized to be an important component of the global carbon cycle (75). In general, higher rates of $^{13}CO_2$ respiration from the labeled amino acids were observed in incubations that contained the added clay minerals compared to the controls, and the correlation of clay minerals with increased ¹³CO₂ respiration was most pronounced in soils where bacteria dominated amino acid assimilation (Fig. 4) and a reduced F:B ¹³C-EAF ratio was observed (Fig. 5). Bacteria have higher amino acid uptake affinity compared to fungi, meaning that bacteria can assimilate amino acids faster at lower concentrations (40). If amino acid sorption onto clay minerals resulted in a lower concentration of bioavailable amino acids (74, 76), bacteria may outcompete fungi leading to higher bacterial EAF values under such conditions. However, under the conditions where bacteria dominated amino acid assimilation (as opposed to fungi), it was relatively inefficient and resulted in increased amino acid remineralization and CO₂ production (Figs. 4 and 5).

Conclusions

Our study shows that fungal:bacterial carbon assimilation ratios are important for carbon stabilization in the early development phase of high-Arctic soils after glacial retreat. Our results link basidiomycete yeasts to this process, identifying them as "pioneer fungi" that likely help in the process of stabilizing organic C in young proglacial soils. These fungi traits will become more important as glaciers continue to retreat in the high-Arctic, and they may also have been important for the recovery of soil ecosystems during past glacial—interglacial cycles in Earth's history.

Materials and Methods

Study Site and Sampling. Our study focuses on the proglacial forefield of Midtre Lovénbreen, a retreating polythermal valley glacier located 5 km South-East of Ny-Ålesund, in North-West Svalbard (78°55' N, 12°45' E; Fig. 1). The annual mean air temperature at the site between 1991 and 2021 was -4.1 ± 1.3 °C with a steady increase over time, and in 2021, the sampling year, the mean annual temperature was 1.2 °C above the 1991 to 2021 average (Norwegian Polar Institute). We selected three main sites of increasing distance from the glacier snout (pioneer, intermediate, and tundra; sites A, B, and C, respectively) for qualitative assessment of vegetation communities (17). These sites serve as a chronosequence representing distinct stages of soil development. We also established a transect between sites A (pioneer soil) and C (tundra) across a distance of 1.2 km in the direction of ice retreat (Fig. 1B), and collected single samples at 40 m intervals along this transect (38 sites in total). We collected surface rock flour sediment or soil (upper 2 cm, excluding conspicuous microbial mats, rocks bigger than 1 cm diameter, and dense radical systems). We also collected supraglacial sediments (muddy ice) from the glacier (ca. 50 m from the snout) in biological

triplicate, and we collected rock flour from the proglacial sediments within five meters of the glacier snout in biological triplicate.

Major geomorphological features along the transect were used to group the samples into the following gradient classes: glacier, snout, early soils, inner moraine, intermediate soils, terminal moraine, and tundra (Figs. 1-3). The oldest soils are at the tundra sites (sites B15-B20 and site C) are outside the terminal moraine, and likely thousands of years old having developed since the end of the last glacial maximum at this site (Fig. 1A). Inside the terminal moraine, the sampled chronosequence corresponds to approximately 120 y of exposure (17) after glacier retreat since the end of the Little Ice Age, represented by the terminal moraine (sites B10-B14) (Fig. 1A). An internal moraine (sites A14-B2) divides the forefield, and seasonal glacier-fed streams also cut through the terrain (sites B8-B10) (Figs. 1 and 2). The map of the sampling area (Fig. 1A) was created using QGIS 3.18 and published estimates of soil age (77), according to geographical data from the Norwegian Polar Institute.

Samples were collected into 15-mL Falcon® tubes using a spatula sterilized with 70% ethanol. With the exception of samples for incubations, samples were frozen within six hours of collection and stored at -20 °C until further processing. The vegetation present at sites A, B, and C and along the transect was qualitatively assessed by examining sites for the presence of various plant species using photographs and field guides (svalbardflora.no; cruise-handbook.npolar.no), in keeping with prior surveys of this chronosequence (17).

Total Adenylate, Total Organic Carbon (TOC), and Total Nitrogen (TN) Measurements. As a proxy for total biomass, we measured total adenylate (ATP+ADP+AMP) concentration from all samples using the "boil and dilute" method described previously (78). In brief, 0.5 g of sample was mixed with 1 mL of sterile MilliQ water and incubated at 99 °C for 10 min. The slurry was centrifuged for 2 min at 13,000 RPM, and total adenylate in the supernatant was measured using a luminometer with the A3 assay according to the manufacturer's instructions (A3 Lucipac, Kikkoman). Relative light units (RLU) were converted to total adenylate concentrations using a standard curve described previously (78). Total nitrogen and carbon % were measured on a CNHS Elemental Analyzer (vario EL cube, Elementar) whereby the total organic carbon % (TOC) was calculated by subtracting the fraction of inorganic carbon from total carbon in the sample, measured using a calcimeter after acidifying the samples with 10% HCl. The detection limits for TOC and TN were 0.05%.

DNA Extraction. We extracted DNA following an established protocol (38). In brief, sediments were transferred to 2-mL Lysing Matrix E tubes (MP Biomedicals, Solon, OH, USA) filled with 1.4 mm ceramic spheres, 0.1 mm silica spheres, and one 4 mm glass sphere. Lysing buffer was prepared containing (for a 50 mL solution) 4 mL of C1 lysing buffer (MoBio, Carlsbad, CA), 0.8 mL 10% SDS, 7.2 mL 100% ethanol, and 38 mL 1 M disodium hydrogen phosphate (Na₂HPO₄). Then, 1 mL of lysing buffer was added to sediment samples in the tubes, and tubes were homogenized for 40 s in a Fast-Prep 5G homogenizer (MP Biomedicals) at 6 m/s. After this step, samples were heated for 2 min at 99 °C and then subject to two freeze–thaw cycles. Samples were later centrifuged for 15 min at 4700 rpm at 24 °C, and the supernatant was purified using the MoBio DNA extraction kit and protocol. For samples with low biomass, near the glacier front, we concentrated the supernatant in Amicon filters (molecular weight cutoff [MWCO] 50 kDa; Millipore) before the purification step. DNA concentration was quantified using the Qubit double-stranded DNA highsensitivity assay kit and a Qubit 3.0 fluorometer (Invitrogen). DNA extractions were finally kept at -20 °C for further analyses.

Stable Isotope Probing Incubation Setup. Sediment or soil was collected from the surface 2 cm of a 2×2 m area applying the same criteria as for the chronosequence sampling. Approximately 500 g of material was collected in a sterilized plastic sealed bag and SIP incubations were started within 12 hrs of sampling. From sites A, B, and C, we incubated 2 g of wet sediment or soil with ¹³C-labeled amino acids (Sigma-Aldrich, Cat# 767964-1EA) and unlabeled amino acids (Sigma-Aldrich, Cat# 79248-5X2ML) as a control. The amino acid mixture consisted of 17 amino acids (alanine, arginine, aspartic acid, glutamic acid, glycine, histidine, isoleucine, leucine, lysine, methionine, phenylalanine, proline, serine, threonine, tyrosine, valine, and cystine), all of which were supplied at 2.5 mM with the exception of cystine that was supplied in the mixture at 1.25 mM. The amino acid mixture was added at a final concentration of 80 μ g g⁻¹, and the samples were incubated in 15-mL Falcon® tubes. We chose to add the amino acids at this concentration because it represents a minor fraction of the naturally existing total organic carbon available to the microbial communities, ca. 0.2 to 1% and 10 to 40% of the TOC and TN, respectively (Fig. 2A). Adding the amino acid substrates at this concentration was intended to reduce "tipping the system" away from the naturally low concentrations of TOC but still provide enough ¹³C-labeled substrate to achieve detectable EAF values in 16S and fungal 18S rRNA genes. Our chosen concentration is within the general concentration range considered to be required for detecting DNA labeling with high-resolution DNA-SIP (62) and is similar to the concentrations of ¹³C-labeled amino acids used by previous DNA-SIP studies to trace bacterial carbon assimilation in agricultural soil (62) and geothermal soils (63).

The addition of the amino acids created a slurry that was gently mixed by pipetting to ensure the substrate was distributed throughout the sediment slurry. Approximately 12 mL of air in the headspace was left to promote aerobic respiration. Tubes were incubated at 4 °C in the dark for either one day or seven days (allowing for two time points) and were terminated by freezing at -20 °C. The glacial forefield where the soils and sediments are located is a hydrologically dynamic environment that exposes sediment and soil microbes to large fluctuations in moisture and so the addition of water to the soil and sediment to create a slurry is reflective of natural conditions.

Clay minerals adsorb organic carbon to their surfaces and therefore restrict bioavailability to soil microbes (74-76). To test the effect of clay minerals on amino acid assimilation (via sorption), we also performed SIP incubations with amino acid clay mineral mixtures. We tested two types of clay minerals with varying structures proposed to be important for organic C sorption (74, 75): kaolinite (a 1:1 clay mineral) and montmorillonite (a 2:1 clay mineral). Unlabeled and labeled amino acids were mixed with 20 mg of kaolinite (Sigma-Aldrich) or montmorillonite (Aldrich, K10) in sterile microfuge tubes and incubated for a 15-d preincubation prior to the addition to soil incubations, to allow time for amino acids to interact with and potentially sorb to clay mineral surfaces before starting the SIP incubations. The amino acid clay mineral mixtures were added to the soil at the same final concentration of amino acids as the controls that contained no additional clay minerals (80 µg/g amino acids). Tubes were incubated under the same conditions as the controls: at 4 °C in the dark for either one day or seven days (allowing for two time points), after which incubations were terminated by freezing at −20 °C.

Ultracentrifugation and Density Gradient Fractionation. Extracted DNA was prepared for density gradient centrifugation following an established qSIP protocol (38, 66, 67). In brief, density gradient centrifugation was performed in a TLN-100 Optima MAX-TL ultracentrifuge (Beckman Coulter, Brea, CA, USA) with a near-vertical rotor at 18 °C for 72 h at 165,000 g. In total, 50 μL of extracted DNA was added to a solution of cesium chloride (CsCl) and gradient buffer (0.1 M Tris, 0.1 M KCl, and 1 mM EDTA) in order to achieve a starting density of 1.71 g/mL in 3.3 mL OptiSeal polyallomer tubes (Beckman Coulter). After ultracentrifugation, density gradients were fractionated into 20 equal fractions of roughly 180 µL from the bottom of OptiSeal polyallomer tubes by using a syringe pump and a fraction recovery system (Beckman Coulter). The refractive index of the fractions was measured immediately after fraction recovery with an AR200 digital refractometer (Reichert Analytical Instruments) and converted to density using a standard curve. After measuring the density of the collected fractions, DNA was precipitated overnight at room temperature using two volumes of polyethylene glycol with 2 µL (20 mg/mL) glycogen. DNA was pelleted via centrifugation (13,000 g, 40 min), washed with 70% ethanol, and resuspended with 30 µL elution buffer (MoBio DNA extraction kit, Qiagen).

qPCR of Bacterial 16S rRNA Genes and Fungal 18S rRNA Genes. qPCR was conducted in a CFX Connect real-time PCR system (Bio-Rad) as described in detail in a previous publication (38). As described previously (38), quantification of prokaryotic 16S rRNA genes was done using the primer pair 515F/806R, whereas fungal 18S rRNA genes were quantified using fungal-specific primers FR1 (5'-AICCATTCAATCGGTAIT-3') and FF390 (5'-CGATAACGAACGAGACCT-3') (79).

16S rRNA Gene and Fungal ITS Sequencing and Analysis. As described previously (80), the 16S ribosomal RNA genes of bacteria and archaea were PCR amplified using the primer pair 515F/806R containing dual-indexed primers. The fungal internal transcribed spacer (ITS) was amplified as described previously (38), with the primer pair ITS1-F/ITS2 (ITS1-F: 5'-CTTGGTCATTTAGAGGAAGTAA-3', ITS2: 5'-GCTGCGTTCTTCATCGATGC-3') that also contained Illumina adapters and a unique barcode sequence for sample demultiplexing. This was determined to capture a realistic picture of fungal OTU richness using fungal mock communities (81). Operational taxonomic units were created using USEARCH (82) as described previously (80, 81). The taxonomic affiliation of the 16S rRNA gene was made as described previously (80) using BLASTn searches of OTU sequences against the SILVA database (83). The ITS taxonomy was assigned as described previously (38) by BLASTn searches of fungal ITS OTUs against the UNITE database release 8 (84).

All 16S and ITS1 rRNA gene sequencing data from the chronosequence have been deposited in the NCBI short read archive database under BioProject ID PRJNA1074128. BioProject PRJNA1074128 also includes all the ITS1 sequencing data from the SIP experiments.

Estimating Excess Atom ¹³C-enrichment Fraction (EAF) of Total 16S and Fungal 18S rRNA Genes. The excess atom fraction ¹³C (EAF) was calculated as a measure of the amount of substrate incorporated into the DNA of either bacteria or fungi from the labeled amino acids. The EAF of bacterial 16S rRNA genes and fungal 18S rRNA genes from the labeled amino acid SIP incubations was calculated as previously described (38) according to the equations for calculating EAF values from DNA-SIP experiments (24). The EAF value should reflect the proportion of labeled carbon atoms that are assimilated into the genomic DNA (or at least large DNA fragments containing rRNA genes). For example, an EAF value of 0.2 would relate to 20% of C atoms within the gene targeted containing the heavier ¹³C isotope (24). When calculating the fungal:bacterial EAF ratio, null results (no detectable labeling) were interpreted as amino acid assimilation being below our EAF detection limit, empirically determined to be 1% (38). This allowed us to calculate a F:B EAF ratio in SIP incubations in cases of no detectable amino acid assimilation.

Measuring Remineralized ¹³C from Amino Acid SIP Incubations. To quantify the remineralization of amino acids added to the SIP incubations, we determined the relative amount of ¹³CO₂ produced using gas chromatography-mass spectrometry (GC-MS) of gas withdrawn from the headspace of incubations. Specifically, 0.2 g of incubation material (muddy slurry) was added to 20 mL gas-tight glass vials that were crimp sealed with gray butyl stoppers, heated to 60 °C for 5 min (in a headspace sampler), and 1 mL of headspace gas was sampled via a headspace autosampler connected to a gas chromatograph with a quadrupole mass spectrometer as the detector (GCMS-QP2020 NX, Shimadzu). N₂ was used as the carrier gas. This GC-MS setup is calibrated for trace gas analysis (H₂, CO, CO₂, and CH₄), by means of a preseparation column [U-Bond, 0.32 mm ID, 10 µm Film, 30 m] to separate larger molecules and a second column [Carboxen-1010 Plot, 0.32 mm ID, 15 μm Film, 30 m] for separating trace gases. The elution time for CO₂ on this particular setup (6.1 minutes) was determined by comparison to a CO₂ standard (99.999% Linde Gas). The relative amount of remineralized carbon from the added labeled amino acids was taken as the percentage of 13 C-labeled CO₂ (m/z = 45) relative to the unlabeled CO_2 (m/z = 44), released from the sample matrix into the flask headspace. These percentages were calculated from the relative abundance of labeled (m/z = 45)and unlabeled (m/z = 44) CO₂, determined via integration of the respective peak areas in the GC-QMS trace. All experimental treatments had ¹³CO₂ percentages higher than the corresponding unlabeled control flasks, which consistently reflected the natural abundance of 13 C in the environment (1.1% \pm 0.05%).

Estimating ¹³C **Assimilation by Specific Fungal Taxa.** In order to quantify amino acid assimilation by specific fungal taxa, SIP incubations showing the highest ¹³C EAF values for fungal 18S rRNA genes (*SI Appendix*, Fig. S2) were selected for fungal ITS1 barcoding of the individual density fractions (resulting from density gradient ultracentrifugation). The two samples that were chosen for fungal-specific Tag-SIP and qSIP were the site A control (no mineral addition), and the tundra (+ montmorillonite) incubations at site C because these represented two end members of the chronosequence which had the highest amount of ¹³C assimilation as evidenced by the EAF of the fungal 18S rRNA genes (*SI Appendix*, Fig. S2). Due to the extremely low fungal biomass at site A (Fig. 2*C*), there was not sufficient material to perform replicates for the site A-control (no mineral addition) incubation.

We therefore could not apply the standard qSIP analysis pipeline (24) for this SIP incubation. Rather, we used the equations from Hungate et al. (24) to calculate the excess atom ^{13}C fraction ("A-values") from buoyant density shifts for each individual OTU in the unlabeled incubations relative to the ^{13}C -labeled incubations. We refer to quantifying the excess atom fraction (EAF) for each OTU present in a single sample as quantitative Tag-SIP (85) or "Tag-qSIP". Tag-qSIP can be described as pseudoquantitative because the relative distribution of ITS1 sequences is quantitatively normalized by the total number of fungal 18S rRNA gene copies determined with qPCR. In the site C (tundra) SIP incubations, the higher fungal biomass was sufficient to perform three replicates for the standard qSIP pipeline. From each incubation fractionation, 12 density fractions in the gradient containing DNA were selected for ITS sequencing following the protocol described above.

The amount of amino acid ¹³C assimilated by specific fungal taxa was calculated based on an isotopic replacement approach which consists of comparing the buoyant density of DNA for a specific OTU in the treatment with labeled amino acids against a control (24). In order to update these calculations for our fungal data, we normalized the fractional sequence abundance of fungal ITS1 OTU sequences using the total concentration of fungal 18S rRNA genes (quantified via qPCR) in the same density fractions. We acknowledge that rRNA operon copy numbers vary between fungal taxa (86) and may bias fungal EAF comparison between different fungal taxa, especially in samples with very different fungal communities. However, this bias should be negligible when comparing EAF of the same fungal OTUs in different samples. The quantitatively normalized fungal ITS1 distributions were then used together with CsCl densities of each fraction to calculate the average buoyant density of each fungal OTU using the same original equations (24) for 16S rRNA genes. These calculations quantify ¹³C incorporation in the DNA of specific taxa and take into account the potential effects of GC content (24). The incorporation of the isotope tracer (13C) is expressed as EAF, which represents the increase above the natural abundance isotopic composition and ranges from 0 to 1 minus the natural abundance background (24). For the tundra incubations, CI of EAF values were calculated as the SD of three replicates (site C). All statistical analyses were performed in R (4.3.1) with RStudio.

Data, Materials, and Software Availability. DNA sequence data have been deposited in NCBI GenBank (PRJNA1074128) (87).

ACKNOWLEDGMENTS. We acknowledge funding from the Deutsche Forschungsgemeinschaft (DFG) through Project OR 417/7-1 (granted to W.D.O.), a NSF-NERC (UKRI) thematic program "Signals in the Soil" (NERC grant: NE/T010967/1; NSF grant: 1935689), and NERC COVID Recovery Support Fund. J.A.B. also acknowledges support from the CNRS Chaires de Professeur Junior (CPJ). We are grateful to the staff of the UK Arctic Research Station and the Ny-Ålesund Research Station-Sverdrup, in Ny-Ålesund, Svalbard, for logistical support in the field. A part of the research was performed in the scope of the Master Program "Geobiology and Paleobiology" (MGAP) at LMU Munich (https://www.mgap.geo.uni-muenchen.de/index.html). We acknowledge the SUN SPEARS 2021 field team and investigators (Trevor P. Irons, Carlos Oroza, Oliver Kuras, Mihai Cimpoiasu, Harry Harrison, Dane Liljestrand, Justin Byington, and Michael Jarzin) for assistance in the field and with funding acquisition.

Author affiliations: ^aDepartment of Earth and Environmental Sciences, Paleontology and Geobiology, Ludwig-Maximilians-Universität München, Munich, Germany, 80333; ^bDepartment of Ecology and Evolutionary Biology, University of Colorado, Boulder, CO 80309; ^cAix Marseille University, University of Toulon, Centre national de la recherche scientifique (CNRS), Institut de Recherche pour le Développement (IRD), Mediterranean Institute of Oceanography (MIO), Marseille, France 13009; ^dSchool of Biological and Behavioural Sciences, Queen Mary University of London, London, United Kingdom, El 4NS; and ^cGeoBio-Center, Ludwig-Maximilians-Universität München, Munich, Germany, 80333

Author contributions: J.C.T.-E., J.P.M.-J., S.K.S., P.S., J.A.B., and W.D.O. designed research; J.C.T.-E., J.P.M.-J., S.K.S., P.S., J.A.B., and W.D.O. performed research; J.C.T.-E., J.P.M.-J., and W.D.O. contributed new reagents/analytic tools; J.C.T.-E., J.P.M.-J., J.A.B. and W.D.O. analyzed data; and J.C.T.-E., P.S., J.A.B., and W.D.O. wrote the paper.

R. Hugonnet et al., Accelerated global glacier mass loss in the early twenty-first century. Nature 592, 726-731 (2021).

R. V. Bekryaev, I. V. Polyakov, V. A. Alexeev, Role of polar amplification in long-term surface air temperature variations and modern arctic warming. J. Clim. 23, 3888–3906 (2010).

F. Pithan, T. Mauritsen, Arctic amplification dominated by temperature feedbacks in contemporary climate models. Nat. Geosci. 7, 181–184 (2014).

B. Noel et al., Low elevation of Svalbard glaciers drives high mass loss variability. Nat. Commun. 11, 4597 (2020).

S. Yoshitake, M. Uchida, Y. Iimura, T. O'htsuka, T. Nakatsubo, Soil microbial succession along a chronosequence on a High Arctic glacier foreland, Ny-Âlesund, Svalbard: 10 years' change. Polar Sci. 16, 59–67 (2018).

S. Cauvy-Fraunie, O. Dangles, A global synthesis of biodiversity responses to glacier retreat. Nat. Ecol. Evol. 3, 1675–1685 (2019).

- R. Wojcik, J. Eichel, J. A. Bradley, L. G. Benning, How allogenic factors affect succession in glacier forefields. Earth-Science Reviews 218, 103642. (2021).
- S. P. Brown, A. Jumpponen, Contrasting primary successional trajectories of fungi and bacteria in retreating glacier soils. Mol. Ecol. 23, 481-497 (2014).
- J. A. Bradley, J. S. Singarayer, A. M. Anesio, Microbial community dynamics in the forefield of glaciers. Proc. Biol. Sci. 281 (2014).
- S. K. Schmidt *et al.*, The earliest stages of ecosystem succession in high-elevation (5000 metres above sea level), recently deglaciated soils. *Proc. Biol. Sci.* **275**, 2793–2802 (2008).
- F. D. Alfaro et al., Soil microbial abundance and activity across forefield glacier chronosequence in the Northern Patagonian Ice Field, Chile. Arctic, Antarctic, and Alpine Research 52, 553–562 (2020).
- S. K. Schmidt et al., Biogeochemical stoichiometry reveals P and N limitation across the post-glacial landscape of Denali National Park. Alaska. Ecosystems 19, 1164–1177 (2016).
- J. L. Darcy et al., Phosphorus, not nitrogen, limits plants and microbial primary producers following glacial retreat. Sci Adv 4, eaaq0942 (2018).
- S. C. Castle et al., Nutrient limitation of soil microbial activity during the earliest stages of ecosystem development. Oecologia 185, 513-524 (2017).
- G. Varliero, A. M. Anesio, G. L. Barker, A taxon-wise insight into rock weathering and nitrogen fixation functional profiles of proglacial systems. Front. Microbiol. 12, 627437. (2021).
- J. Knelman, S. K. Schmidt, G. E. B., Cyanobacteria in early soil development of deglaciated forefields: Dominance of non-heterocystous filamentous cyanobacteria and phosphorus limitation of N-fixing Nostocales. Soil Biol. Biochem. 154, 108127. (2021).
- I. D. Hodkinson, S. J. Coulson, N. R. Webb, Community assembly along proglacial chronosequences in the high Arctic: vegetation and soil development in north-west Svalbard. *J. Ecol.* **91**, 651–663 (2003).
- J. A. Bradley, Microbial Life in the Cryosphere and its Feedback on Global Change, S. Liebner, L. 18. Ganzert, Eds. (de Gruyter, Berlin, Boston, 2021), pp. 253-264.
- P. F. Hoffman et al., Snowball Earth climate dynamics and Cryogenian geology-geobiology. Sci. Adv. 3, e1600983 (2017).
- G. Gleixner, Soil organic matter dynamics: a biological perspective derived from the use of compound-specific isotopes studies. Ecol. Res. 28, 683-695 (2013).
- J. P. Schimel, S. M. Schaeffer, Microbial control over carbon cycling in soil. Front. Microbiol. 3, 348 (2012).
- F. Tao et al., Microbial carbon use efficiency promotes global soil carbon storage. Nature 618, 981-985 (2023).
- P. Dijkstra et al., Modeling soil metabolic processes using isotopologue pairs of position-specific 13CC-labeled glucose and pyruvate. Soil Biol. Biochem. 43, 1848-1857 (2011).
- B. A. Hungate et al., Quantitative microbial ecology through stable isotope probing. Appl. Environ. Microbiol. 81, 7570-7581 (2015).
- 25. Y. Sakata-Bekku, T. Nakatsubo, A. Kume, H. Koizumi, Soil microbial biomass, respiration rate, and temperature dependence on a successional glacier foreland in Ny-Ålesund, Svalbard. Arctic, Antarctic, and Alpine Research 34, 395-399 (2004).
- K. K. Treseder, J. T. Lennon, Fungal traits that drive ecosystem dynamics on land. Microbiol. Mol. Biol. Rev. 79, 243-262 (2015).
- 27. A. A. Malik et al., Soil fungal: Bacterial ratios are linked to altered carbon cycling. Front. Microbiol. 7, 1247 (2016).
- $M.\,S.\,Strickland,\,J.\,Rousk,\,Considering\,\,fungal: bacterial\,\,dominance\,\,in\,\,soils\,\,-\,\,Methods,\,controls,\,and\,\,dominance\,\,in\,\,soils\,\,-\,\,Methods,\,controls,\,and\,\,dominance\,\,in\,\,soils\,\,-\,\,Methods,\,controls,\,and\,\,dominance\,\,in\,\,soils\,\,-\,\,Methods,\,controls,\,and\,\,dominance\,\,in\,\,soils\,\,-\,\,Methods,\,controls,\,and\,\,dominance\,\,in\,\,soils\,\,-\,\,Methods,\,controls,\,and\,\,dominance\,\,in\,\,soils\,\,-\,\,Methods,\,controls,\,and\,\,dominance\,\,in\,\,soils\,\,-\,\,Methods,\,controls,\,and\,\,dominance\,\,in\,\,soils\,\,-\,\,Methods,\,controls,\,and\,\,dominance\,\,in\,\,soils\,\,-\,\,Methods,\,controls,\,and\,\,dominance\,\,in\,\,soils\,\,-\,\,Methods,\,controls,\,and\,\,dominance\,\,in\,\,soils\,\,-\,\,Methods,\,controls,\,and\,\,dominance\,\,in\,\,soils\,\,-\,\,Methods,\,controls,\,and\,\,dominance\,\,in\,\,soils\,\,-\,\,Methods,\,controls,\,and\,\,dominance\,\,in\,\,soils\,\,-\,\,Methods,\,controls,\,and\,\,dominance\,\,in\,\,soils\,\,-\,\,Methods,\,controls,\,and\,\,dominance\,\,in\,\,soils\,\,-\,\,Methods,\,controls,\,and\,\,dominance\,\,in\,\,soils\,\,-\,\,Methods,\,and\,\,dominance\,\,in\,\,soils\,\,-\,\,Methods,\,and\,\,dominance\,\,in\,\,soils\,\,-\,\,Methods,\,and\,\,dominance\,\,in\,\,soils\,\,-\,\,Methods,\,and\,\,dominance\,\,in\,\,soils\,\,-\,\,Methods,\,and\,\,dominance\,\,in\,\,soils\,\,-\,\,Methods,\,and\,\,dominance\,\,in\,\,soils\,\,-\,\,Methods,\,and\,\,dominance\,\,in\,\,soils\,\,-\,\,Methods,\,and\,\,dominance\,\,in\,\,soils\,\,-\,\,Methods,\,and\,\,dominance\,\,in\,\,soils\,\,-\,\,Methods,\,and\,\,dominance\,\,in\,\,soils\,\,-\,\,Methods,\,and\,\,dominance\,\,in\,\,soils\,\,-\,\,Methods,\,and\,\,dominance\,\,in\,\,soils\,\,-\,\,Methods,\,and\,\,dominance\,\,in\,\,soils\,\,-\,\,Methods,\,and\,\,dominance\,\,in\,\,soils\,\,-\,\,Methods,\,and\,\,dominance\,\,in\,\,soils\,\,-\,\,Methods,\,and\,\,dominance\,\,in\,\,soils\,\,-\,\,Methods,\,and\,\,dominance\,\,in\,\,soils\,\,-\,\,Methods,\,and\,\,dominance\,\,in\,\,soils\,\,-\,Methods,\,and\,\,dominance\,\,in\,\,soils\,\,-\,Methods,\,and\,\,dominance\,\,in\,\,soils\,\,-\,Methods,\,and\,\,dominance\,\,in\,\,soils\,\,-\,Methods,\,and\,\,dominance\,\,in\,\,soils\,\,-\,Methods,\,and\,\,dominance\,\,in\,\,soils\,\,-\,Methods,\,and\,\,dominance\,\,in\,\,soils\,\,-\,Methods,\,and\,\,dominance\,\,in\,\,soils\,\,-\,Methods,\,and\,\,dominance\,\,in\,\,soils\,\,-\,Methods,\,and\,\,dominance\,\,in\,\,soils\,\,-\,Methods,\,and\,\,dominance\,\,in\,\,soils\,\,-\,Methods,\,and\,\,dominance\,\,in\,\,soils\,\,-\,Methods$ ecosystem implications. Soil. Biol. Biochem. 42, 1385-1395 (2010).
- R. L. Sinsabaugh, S. Manzoni, D. L. Moorehead, A. Richter, Carbon use efficiency of microbial communities: Stoichiometry, methodology and modelling. Ecol. Lett. 16, 930-939 (2013).
- J. Fabian, S. Zlatanovic, M. Mutz, K. Premke, Fungal-bacterial dynamics and their contribution to terrigenous carbon turnover in relation to organic matter quality. ISME J. 11, 415-425 (2017).
- 31. V. L. Bailey, J. L. Smith, H. Bolton, Fungal-to-bacterial ratios in soils investigated for enhanced C sequestration. Soil. Biol. Biochem. 34, 997-1007 (2002).
- R. D. Bardgett, P. J. Hobbs, Å. Frostegård, Changes in soil fungal:bacterial biomass ratios following reductions in the intensity of management of an upland grassland. *Biol. Fertil. Soils* **22**, 261–264 (1996).
- J. Six, S. D. Frey, R. K. Thiet, K. M. Batten, Bacterial and fungal contributions to carbon sequestration in agroecosystems. Soil. Sci. Soc. Am. J. 70, 555-569 (2006).
- B. G. Waring, C. Averill, C. Hawkes, Differences in fungal and bacterial physiology alter soil carbon and nitrogen cycling: Insights from meta-analysis and theoretical models. *Ecol. Lett.* **16**, 887-894 (2013).
- V. de Garcia, S. Brizzio, D. Libkind, P. Buzzini, M. van Broock, Biodiversity of cold-adapted yeasts from glacial meltwater rivers in Patagonia, Argentina. *FEMS Microbiol. Ecol.* **59**, 331–341 (2007).
- P. Dresch et al., Emerging from the ice-fungal communities are diverse and dynamic in earliest soil developmental stages of a receding glacier. Environ. Microbiol. 21, 1864-1880 (2019).
- L. Tedersoo et al., Fungal biogeography. Global diversity and geography of soil fungi. Science 346, 1256688 (2014).
- W. D. Orsi et al., Carbon assimilating fungi from surface ocean to subseafloor revealed by coupled phylogenetic and stable isotope analysis. ISME J. 16, 1245-1261 (2022).
- P. L. Sorensen, A. Michelsen, I. Jonassen, Ecosystem partitioning of 15N-glycine after long-term climate and nutrient manipulations, plant clipping and addition of labile carbon in a subarctic heath tundra. Soil. Biol. Biochem. 40, 2344-2350 (2008).
- J. Hobbie, J. Hobbie, Amino acid cycling in plankton and soil microbes studied with radioisotopes: measured amino acids in soil do not reflect bioavailability. *Biogeochemistry* **107**, 339–360 (2012).
- 41. A. Nordin, I. K. Schmidt, G. R. Shaver, Nitrogen uptake by arctic soil microbes and plants in relation to soil nitrogen supply. Ecology 85, 955-962 (2004).
- B. G. Pautler *et al.*, Molecular characterization of dissolved organic matter in glacial ice: coupling natural abundance 1H NMR and fluorescence spectroscopy. Environ. Sci. Technol. 46, 3753-3761 (2012).
- M. Kida et al., Dissolved Organic Matter Processing in Pristine Antarctic Streams. Environ. Sci. Technol. 55, 10175-10185 (2021).
- J. Bradley et al., Microbial dynamics in a High-Arctic glacier forefield: a combined field, laboratory, and modelling approach. Biogeosciences 13, 5677-5696 (2016).
- S. Yoshitake, M. Uchida, H. Koizumi, T. Nakatsubo, Carbon and nitrogen limitation of soil microbial respiration in a High Arctic successional glacier foreland near Ny-Ålesund. Svalbard. Polar Res. 26,
- Y. Liu et al., Plant colonization mediates the microbial community dynamics in glacier forelands of the Tibetan Plateau. iMeta 2, e91. (2023).
- F. A. Thomas, R. K. Sinha, K. P. Krishnan, Bacterial community structure of a glacio-marine system in the Arctic (Ny-Ålesund, Svalbard). Sci. Total Environ. 20, 135264. (2020).
- W. Hu, S. K. Schmidt, P. Sommers, J. L. Darcy, D. L. Porazinska, Multiple-trophic patterns of primary succession following retreat of a high-elevation glacier. Ecosphere 12, e03400. (2021).

- 49. C. L. Schoch et al., Nuclear ribosomal internal transcribed spacer (ITS) region as a universal DNA barcode marker for Fungi. Proc. Natl. Acad. Sci. U.S.A. 16 (2012).
- R. A. Duo Saito et al., Metabarcoding analysis of the fungal biodiversity associated with Castaño Overa glacier - Mount Tronador, Patagonia, Argentina. Fungal Ecol. 36, 8-16 (2018).
- L. Perini, K. Andrejasic, C. Gostincar, N. Gunde-Cimerman, P. Zalar, Greenland and Svalbard glaciers host unknown basidiomycetes: the yeast Camptobasidium arcticum sp. nov. and the dimorphic Psychromyces glacialis gen. and sp. nov. Int. J. Syst. Evol. Microbiol. 71 (2021).
- L. Perini et al., Darkening of the Greenland Ice Sheet: Fungal Abundance and Diversity Are Associated With Algal Bloom. Front. Microbiol. 10, 557 (2019).
- L. Perini, C. Gostincar, N. Gunde-Cimerman, Fungal and bacterial diversity of Svalbard subglacial ice. Sci. Rep. 9, 20230 (2019).
- P. Buzzini, M. Turk, L. Perini, B. Turchetti, N., Gunde-Cimerman in *Yeasts in Natural Ecosystems*, P. Buzzini, M. A. Lachance, A. Yurkov, Eds. (Springer, Cham, 2017), pp. 331–365. 54.
- A. Edwards et al., A distinctive fungal community inhabiting cryoconite holes on glaciers in Svalbard. Fungal Ecol. 6, 168-176 (2013).
- B. Luo et al., Habitat-specificity and diversity of culturable cold-adapted yeasts of a cold-based glacier in the Tianshan Mountains, northwestern China. Appl. Microbiol. Biotechnol. 103, 2311-2327 (2019).
- V. de Garcia, P. Zalar, S. Brizzio, N. Gunde-Cimerman, M. van Broock, Cryptococcus species (Tremellales) from glacial biomes in the southern (Patagonia) and northern (Svalbard) hemispheres. FEMS Microbiol. Ecol. 82, 523-539 (2012).
- C. Coleine, J. E. Stajich, L. Selbmann, Fungi are key players in extreme ecosystems. Trends Ecol. Evol **37**, 517-528 (2022).
- J. Tian et al., Ecological Succession Pattern of Fungal Community in Soil along a Retreating Glacier. Front. Microbiol. 8, 1028 (2017).
- P. Vinšová et al., The biogeochemical legacy of arctic subglacial sediments exposed by glacier retreat. Global Biogeochem. Cycles 36, e2021GB007126 (2022).
- J. A. Bradley et al., Active and dormant microorganisms on glacier surfaces. Geobiology 21, 244-261 (2023).
- I. J. Klarenberg, C. Keuschnig, A. Salazar, L. G. Benning, O. Vilhelmsson, Moss and underlying soil bacterial community structures are linked to moss functional traits. Ecosphere 14, e4447. (2023).
- S. E. Barnett, N. D. Youngblut, C. N. Koechli, D. H. Buckley, Multisubstrate DNA stable isotope probing reveals guild structure of bacteria that mediate soil carbon cycling. Proc. Natl. Acad. Sci. U.S.A. 118 (2021).
- D. Lai et al., Resource partitioning and amino acid assimilation in a terrestrial geothermal spring. ISME J. 17, 2112-2122 (2023).
- A. L. Robinson, N. Deluigi, C. Rolland, N. Manetti, T. Battin, Glacier loss and vegetation expansion alter organic and inorganic carbon dynamics in high-mountain streams. Biogeosciences 20, 2301-2316 (2023).
- O. K. Coskun et al., Quantifying the effects of hydrogen on carbon assimilation in a seafloor microbial community associated with ultramafic rocks. ISME J. 16, 257-271 (2022).
- O. K. Coskun et al., Quantifying genome specific carbon fixation in a 750 meter deep subsurface hydrothermal microbial community. FEMS Microbiology Ecology fiae062, (2024), doi.org/10.1093/ femsec/fiae062.
- G. S. de Hoog, The Black Yeasts, II: Moniliella and Allied Genera. Studies in mycology; no. 19 (Centraalbureau voor Schimmelcultures, 1979).
- C. A. Rosa et al., Synonymy of the yeast genera Moniliella and Trichosporonoides and proposal of Moniliella fonsecae sp. nov. and five new species combinations. Int. J. Syst. 59 (2009), doi. org/10.1099/ijs.0.065117-0.
- G. S. de Hoog, M. T. Smith, C. A., in Rosa, C. P. The Yeasts, J. W. Kurtzman, T. Boekhout. Fell, Eds. (Elsevier, 2011), pp. 1837-1846.
- S. Ruisi, D. Barreca, L. Selbmann, L. Zucconi, S. Onofri, Fungi in Antarctica. Rev. Environ. Sci. Biotechnol. 6, 127-141 (2007).
- F. Maillard et al., Melanization slows the rapid movement of fungal necromass carbon and nitrogen into both bacterial and fungal decomposer communities and soils. mSystems 8, e0039023. (2023).
- S. R. Thomas-Hall et al., Cold-adapted yeasts from Antarctica and the Italian Alps-description of three novel species: Mrakia robertii sp. nov., Mrakia blollopis sp. nov. and Mrakiella niccombsii sp. nov. Extremophiles 14, 47-59 (2010).
- M. Kleber et al., Dynamic interactions at the mineral-organic matter interface. Nat. Rev. Earth & Environ. 2, 402-421 (2021).
- J. D. Hemingway et al., Mineral protection regulates long-term global preservation of natural organic carbon. Nature 570, 228-231 (2019).
- W. Szymański et al., Occurrence and stability of organic intercalation in clay minerals from permafrost-affected soils in the High Arctic-A case study from Spitsbergen (Svalbard). Geoderma **408**, 115591 (2022).
- M. Bourriquen et al., Paraglacial coasts responses to glacier retreat and associated shifts in river floodplains over decadal timescales. Land Degradation & Development 29, 4173-4185 (2018).
- W. D. Orsi, A rapid method for measuring ATP + ADP + AMP in marine sediment Environ. Microbiol. **25**, 1549-1558 (2023).
- N. Chemidlin Prevost-Boure et al., Validation and application of a PCR primer set to quantify fungal communities in the soil environment by real-time quantitative PCR. PLoS One 6, e24166. (2011).
- M. Pichler et al., A 16S rRNA gene sequencing and analysis protocol for the Illumina MiniSeq
- platform. *Microbiologyopen* **7**, e00611. (2018).

 A. S. Ortega-Arbulu, M. Pichler, A. Vuillemin, W. D. Orsi, Effects of organic matter and low oxygen on the mycobenthos in a coastal lagoon. Environ. Microbiol. 21, 374-388 (2019).
- R. C. Edgar, UPARSE: highly accurate OTU sequences from microbial amplicon reads. Nat. Methods 10, 996-998 (2013).
- C. Quast et al., The SILVA ribosomal RNA gene database project: improved data processing and web-based tools. Nucleic Acids Res. 41, D590-596 (2013).
- R. H. Nilsson et al., The UNITE database for molecular identification of fungi: handling dark taxa and parallel taxonomic classifications. Nucleic Acids Res. 47, D259-D264 (2019).
- W. D. Orsi et al., Diverse, uncultivated bacteria and archaea underlying the cycling of dissolved protein in the ocean. ISME J. 10, 2158-2173 (2016).
- L. A. Lofgren et al., Genome-based estimates of fungal rDNA copy number variation across phylogenetic scales and ecological lifestyles. Mol. Ecol. 28, 721-730 (2018).
- J. C. Trejos-Espeleta et al., Data from "Raw 16S rRNA gene and ITS1 fungal amplicon sequences from Illumina of an Arctic proglacial soil chronosequence." NCBI. Available at https://www.ncbi.nlm. nih.gov/bioproject/?term=1074128. Deposited 1 March 2024.